ISSN 0016-7932, Geomagnetism and Aeronomy, 2019, Vol. 59, No. 1, pp. 35–44. © Pleiades Publishing, Ltd., 2019.
Russian Text © B.V. Dovbnya, B.I. Klain, N.A. Kurazhkovskaya, 2019, published in Geomagnetizm i Aeronomiya, 2019, Vol. 59, No. 1, pp. 39–49.

Dynamics of Ionospheric Alfvén Resonances from the End of Cycle 21 through Cycle 24 of Solar Activity

B. V. Dovbnya[a, *], B. I. Klain[a, **], and N. A. Kurazhkovskaya[a, *]**

[a]*Borok Geophysical Observatory, Branch of Schmidt Institute of Physics of the Earth, Russian Academy of Sciences, Borok, Yaroslavl oblast, 152742 Russia*

**e-mail: dovbnya@inbox.ru*

***e-mail: klain@borok.yar.ru*

****e-mail: knady@borok.yar.ru*

Received February 5, 2018; revised February 20, 2018; accepted September 27, 2018

Abstract—The results of the study of the dynamics of ionospheric Alfvén resonances (IARs) in a range of 0–10 Hz based on data from magnetic field observations at the midlatitude Borok observatory ($L = 2.8$) from the end of solar cycle 21 through solar cycle 24 are presented. It is shown that IARs in 30% of events are accompanied by the simultaneous observation of structured *Pc*1 geomagnetic pulsations ("pearls") and IARs are recorded in 70% of events without *Pc*1 excitation. A specific feature of pearls is that they are observed predominantly at a frequency of the IAR first resonance band. The qualitative coincidence of the dynamics of frequencies of IAR and *Pc*1 wave packets is detected in 80% of events. The probability maximum of IAR observation falls in the hours before midnight (2000–2200 MLT). IAR seasonal variation is characterized by the presence of two equinoctial maxima. It is shown that the 11-year variation in the IAR emission is controlled by the dynamics of some parameters of the solar wind and IMF. The probability of IAR observation is maximal (in years of solar activity minima) when the ratio of the proton density to the helium ion (α particle) density Np/Na (we note that it is customary to use the inverse, i.e., Na/Np, for the solar wind) and parameter β (which characterizes the ratio of thermal pressure to magnetic pressure) reach the maximum values, while the dynamic pressure of solar wind P_{dyn} (which controls the magnetosphere compression) is decreased. The coincidence of the dynamics of the frequencies of the IAR first resonance band and pearls, as well as of their seasonal and cyclic variations, may be evidence of the interrelation of these oscillatory processes and the possible common mechanism of their generation.

DOI: 10.1134/S0016793219010067

1. INTRODUCTION

In recent years, the study of the so-called ionospheric Alfvén resonances (IARs) has provoked great interest, e.g., (Dovbnya et al., 2013; Baru et al., 2014; Dudkin et al., 2014; Surkov and Hayakawa, 2014; Polyushkina et al., 2015; Potapov et al., 2016). For the first time, the possibility of the existence of a resonator for Alfvén waves in the ionosphere, which was termed "ionospheric Alfvén resonator," was shown theoretically (Polyalov and Rapoport, 1981). The detection of resonance structures in the spectrum of natural electromagnetic noise was experimental confirmation of the existence of the IAR (Belyaev et al., 1987). A multitude of domestic and foreign publications on experimental and theoretical IAR studies appeared later (Belyaev et al., 1989a, 1989b, 1999, 2000; Bosinger et al., 2002; Baru et al., 2013; Surkov and Hayakawa, 2014; Polyushkina et al., 2015). In addition, attempts to study IAR based on satellite observations were made (Dudkin et al., 2014). In these and some other works, morphologically specific IAR features are described in detail.

On dynamic spectra, typical IARs have the form of discrete spectral structures in a frequency range of 0–10 Hz. Their main characteristics are a probability of the observation and frequency of spectral bands. As usual, IARs arise during quiet or moderate geomagnetic activity (Yahnin et al., 2003). It is known that IARs are observed within a wide range of geomagnetic latitudes, e.g., low (Bosinger et al., 2002), middle (Polyushkina et al., 2015), and high (Belyaev et al., 1999) latitudes. The maximal IAR observation probability falls on the local midnight (Baru et al., 2013). Concerning IAR seasonal variation, contradictory information exists in the literature. Thus, for the seasonal variation in a frequency of spectral bands and for their observation time, a maximum at the winter solstice is typical (Yahnin et al., 2003; Baru et al., 2013; Polyushkina et al., 2015). The probability of recording IAR in the winter season is also great (Baru et al., 2013). However, Polyushkina et al. (2015) did not find a dependence of IAR observation probability on the season. Analysis of IAR statistics showed that they are recorded mainly in years of solar activity minima (Belyaev et al., 2000; Baru et al., 2014).

Many researchers note that IAR regularities are closely related to the local ionospheric state. Thus, Polyushkina et al. (2015) revealed a correlation of diurnal and seasonal variations in the frequency of resonance bands with changes in the critical frequency of the ionosphere *foF*2. It was shown (Baru et al., 2014) that there is an inverse dependence between the IAR variation in the solar cycle and the behavior of the critical frequency of the ionospheric layer F_2.

A few alternate mechanisms for the excitation of spectral resonance structures (due to which they emerge) is discussed in the literature, e.g., thunderstorm activity in equatorial regions (Belayev et al., 1989a), plasma instabilities (feedback instability) (Lysak, 1991; Pokhotelov et al., 2001), ionospheric neutral winds (Surkov et al., 2004), etc. This fact shows that the question of the IAR source has not been finally settled and encourages further research on this phenomenon.

It should be noted that the response of IAR characteristics, mainly, to local ionospheric parameters is considered in all studies. At the same time, the influence of global processes on regularities of IAR excitation is little discussed in the literature. An exception is the work by Guglielmi and Potapov (2017), who studied the magnetic field effect on IAR diurnal activity. It is assumed that IARs are purely ionospheric phenomenon. However, it was noted earlier (Dovbnya et al., 2012, 2014) that emissions having a resonance structure of the spectrum of the Alfvén resonator may in some cases be accompanied by a series of structured *Pc*1 geomagnetic pulsations, called "pearls" (string of pearls). Each *Pc*1 series consists of a sequence of wave packets within a frequency range of 0.2–5.0 Hz that recur at predefined intervals. The characteristic amplitude modulation of pearls is clearly seen on magnetograms, while their dynamic spectra have a specific structure (Guglielmi and Troitskaya, 1973). It is known that the *Pc*1 geomagnetic pulsations relate to internal magnetospheric processes, and their excitation in many respects is determined by the interaction between the solar wind and the Earth's magnetosphere. Thus, studies of the effect of interplanetary medium parameters on the processes of exciting IARs, the generation of which may be interrelated with excitation of *Pc*1 geomagnetic pulsations, are of interest.

In this work, the regularities of diurnal, seasonal, and cyclic variations in the probability of observation of IAR emission from the end of solar cycle 21 through solar cycle 24 are studied, and the parameters of the solar wind and interplanetary magnetic field (IMF) that control the dynamics of midlatitude IARs were sought.

2. EXPERIMENTAL DATA

In this work, data from recordings of the magnetic field at the midlatitude Borok Geophysical Observatory of the Institute of Physics of the Earth of the Russian Academy of Sciences (Borok GO of IPE RAS) were used as the initial material: the corrected geomagnetic coordinates $\Phi = 53.6°$; $\Lambda = 114.4°$, $L = 2.8$ for two periods of observation (1984–1993 and 1997–2016). Analysis of the first observation period was conducted with ultralow-frequency (ULF) emission records produced by an analog tape-recorder from an induction magnetometer (data from the archive of the Borok GO of IPE RAS). The analog records were previously presented in digital form; their spectral–temporal analysis was then performed, as a result of which the dynamic spectra of ULF pulsations were obtained. Materials of the second observation period are taken from the database of the Information-measuring complex of the Borok GO of IPE RAS (geodata.borok.ru). The dynamic spectra of ULF pulsations obtained from continuous digital recording of the geomagnetic field were presented in this open-access database (up to 2017, wwwbrk.adm.yar.ru), which allowed observable IARs to be identified.

Analyzing visually the dynamic spectra of ULF emissions, we formed a sampling of the mid-latitude IAR observations for further research. For the first period (1984–1993), 1314 days of IAR observation were selected; for the second period (1997–2016), 1470 days were chosen. Thus, a total of 2784 days for which the spectral resonance structures were identified were analyzed.

The sampling of pearl observations was composed additionally. For this purpose, the dynamic spectra of ULF pulsations were analyzed for the same observation intervals as IAR observations. Apart from this, magnetograms with a high sensitivity of 0.01 nT/mm and the sweeping of 30 mm/min (data from the archive of the Borok GO of IPE RAS) were used. A total of 1800 days of pearl recording were selected for a period of 1984–2016.

The 27-day average values of the Wolf numbers and the parameters of the solar-wind plasma and IMF presented in the OMNI database (http://omniweb.gsfc.nasa.gov/ow.html), were used to analyze interplanetary conditions. From these data, we derived the annual-average values of Wolf numbers and main interplanetary parameters for two analyzed intervals (1984–1993 and 1997–2016). Since there were omissions in dynamic spectra from 1994 up to 1996, at some research stages, we separately considered the IAR dynamics in solar cycles 21–22 (1984–1993) and in 23–24 (1997–2016).

3. RESEARCH RESULTS

3.1. Morphological Specific Features of Analyzed IAR Radiations

As a result of the analysis of dynamic spectra of ULF pulsations, it was detected that the IAR emissions in 30% of events were observed synchronously with the excitation of structured *Pc*1 geomagnetic pulsations, which are called "pearls." Here, we note that two types of pulsations—structured and unstructured—are marked in a range of *Pc*1 frequencies; each of them has specific regularities (Kerttula et al., 2001; Parkhomov et al., 2013). In 70% of events, the IARs were observed without the presence of pearls. Below, for brevity, we use the abbreviation "*Pc*1" to indicate pearls (structured *Pc*1 pulsations).

We divided the initial data conventionally into two groups: (1) IARs (1951 observation days); and (2) IARs accompanied by pearls (833 observation days). Figure 1 presents typical examples of the dynamical spectra of (a) IARs and (b, c) IARs accompanied by *Pc*1 excitation, based on the data from Borok observatory. The bottom parts of Figs. 1b and 1c give the observed wave packets of pearls in expanded form. It can be seen that the frequency of discrete spectral bands begins growing gradually in the afternoon or evening time, reaching a maximum near midnight, and then smoothly decreases toward the postmidnight and morning hours (Fig. 1a). A similar behavior of the frequency of IAR radiation bands within 24 h was noted by many authors, e.g., (Dovbnya et al., 2013; Baru et al., 2013; Polyushkina et al., 2015). The frequency of bands of IARs accompanied by excitation of *Pc*1 pulsations behaves in a similar way (Figs. 1b, 1c). However, in contrast to the events of the first group, sequences of individual wave packets of pearls can be seen on the IAR spectral bands. Pearls may emerge sometimes at the frequency of the second, third, and other spectral bands (see Fig. 1b), but they appear at the frequency of the first spectral band in dominant number of occurrences (Fig. 1c). Moreover, the frequency of these packets changes synchronously with the dynamics of the first IAR harmonic frequency (Fig. 1c). This trend toward gradual growth in the frequency of the first IAR spectral band and pearl frequency is noted in about 80% of the 833 analyzed occurrences.

Figure 2 presents the distributions of the IAR duration (t) of two groups obtained based on data from observations for a period of 1984–1993. The dynamic spectra of ULF pulsations for this time interval had a relatively high resolution in comparison to that in the period 1997–2016 and allowed better identification of the time intervals during which spectral bands were observed. It can be seen that the shapes of the obtained distributions differ substantially. Thus, the duration of the first-group IAR changes within a range of 2–16 h with an average and median value of 9 h (Fig. 2a). Emissions of the IARs accompanied by pearls can last from 2 to 25 or more h (Fig. 2b). The average and median value of the duration of the second-group of IAR emission is 16 h. It can be seen that the duration distribution of spectral bands relating to the second group has a long tail in contrast to the t distribution of the first group. In the dominant number of occurrences, the emission duration of the IARs of the first and second groups is $t \sim 6$–8 h and $t \sim 14$–18 h, respectively. Thus, the observation duration of IARs accompanied by pearl excitation is considerably greater than the observation duration of the IARs without pearls.

3.2. Diurnal Variation in the Number of Events of Observations of Two IAR Groups

The diurnal variation in the probability of observation of two IAR groups was constructed based on observational data from the period of 1984–1993 and on the same considerations mentioned in section 3.1. Since the spectral resonance bands were observed continuously during long-term time intervals, in order to construct the dependence of the IAR observation probability on the local time, we divided (in each group of IAR) the time of their recording into hourly intervals. For convenience in comparing the diurnal variations in emissions of two IAR groups, the number of occurrences in each hourly interval was normalized to their maximum number. Figure 3 demonstrates the diurnal variation in the normalized number of the emission observation occurrences N/N_{max} of (a) IARs and (b) IARs accompanied by pearls. It can be seen that the maximum of the observation probability of the IARs relating to both first and second groups falls in the premidnight hours (2000–2200 MLT). However, the shapes of the obtained distributions have certain differences. Thus, there are no spectral bands near the noon meridian in the diurnal behavior of IAR emission, whereas spectral bands are observed on all days in the diurnal variation of IARs accompanied by pearls. In addition, in the diurnal distribution of the second-group IARs, a small maximum of the observation probability is seen near the noon (Fig. 3b).

3.3. Seasonal Variation in the Number of Events of Observations of Two IAR Groups

In the construction of the seasonal variation for IAR emissions, the number observation days N in each month served as the main characteristic. Figure 4 presents the seasonal variation in the number of occurrences of (a) IARs and (b) IARs accompanied by excitation of *Pc*1 pulsations. It can be seen that the seasonal variations in emissions of two IAR groups have a similar form. The maximum of the probability of observation of two IAR groups falls in the season of the spring (March) and autumnal (September) equinoxes. Here, it should be noted that our obtained seasonal variation in IAR observation probability differs fundamentally from the

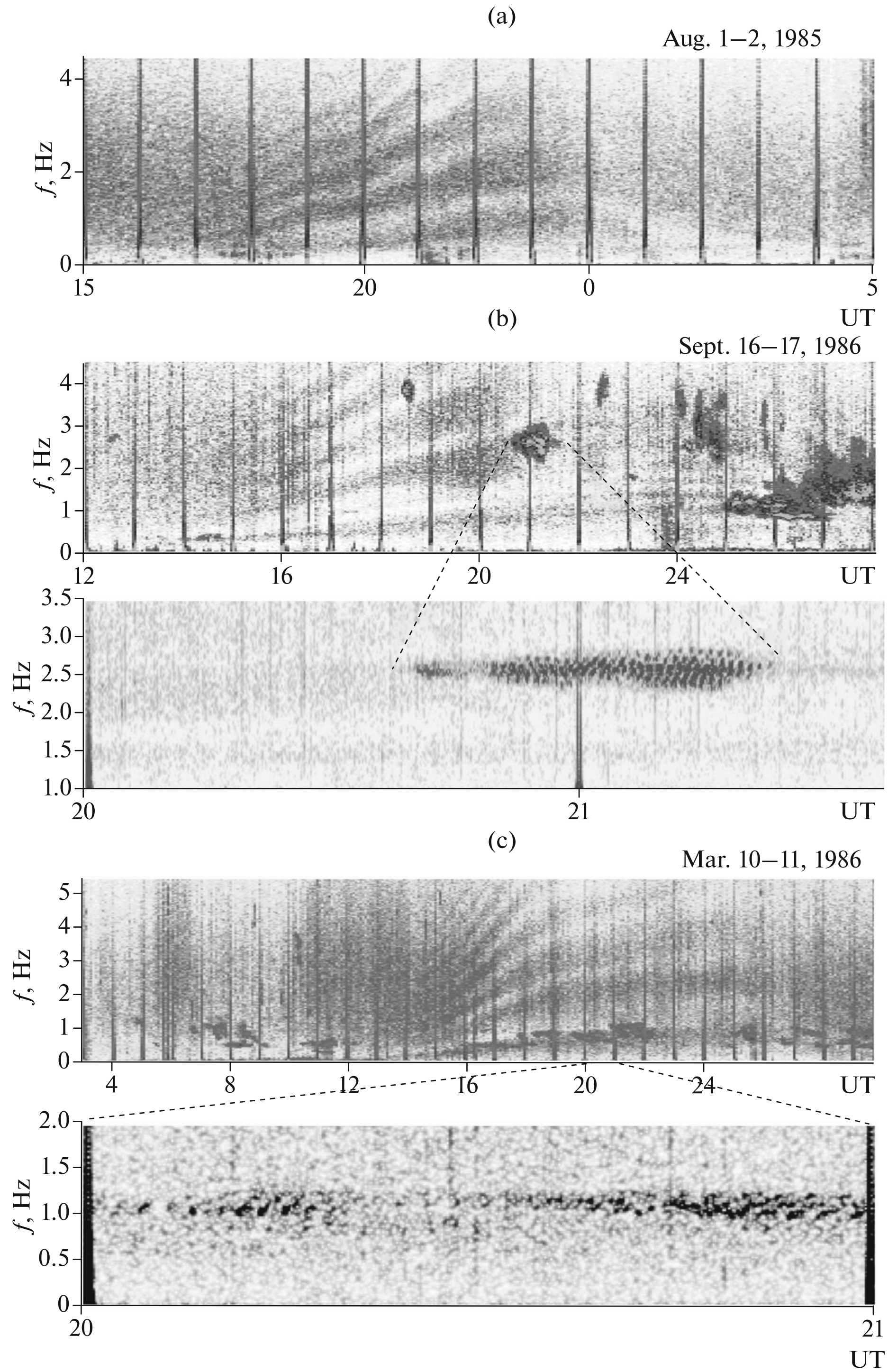

Fig. 1. Typical examples of observation of (a) the IAR on August 1–2, 1985, and (b, c) the pearl-accompanied IAR on (b) September 16–17, 1986, and (c) March 10–11, 1986, at the midlatitude Borok observatory. Bottom of panels b and c: pearls are presented in expanded form.

seasonal variation obtained by other researchers. Thus, Baru et al. (2013) concluded that the resonance structures of the spectrum are observed mainly in winter. According to data (Polyushkina et al., 2015), the emergence of resonance structures is independent of the season.

3.4. Cyclic Variation in the Number of Events of Observations of Two IAR Groups and Its Relation to Interplanetary Medium Parameters

Such a large data array made it possible to consider not only the seasonal but also cyclic dynamics of IAR

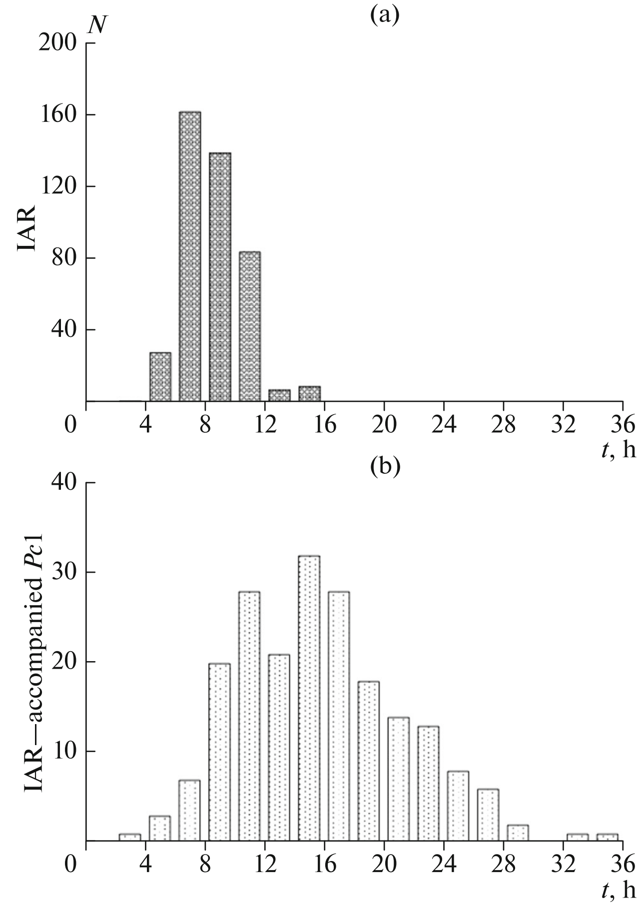

Fig. 2. Histograms of distributions of emission duration t of (a) IAR and (b) IARs accompanied by excitation of *Pc*1 pulsations.

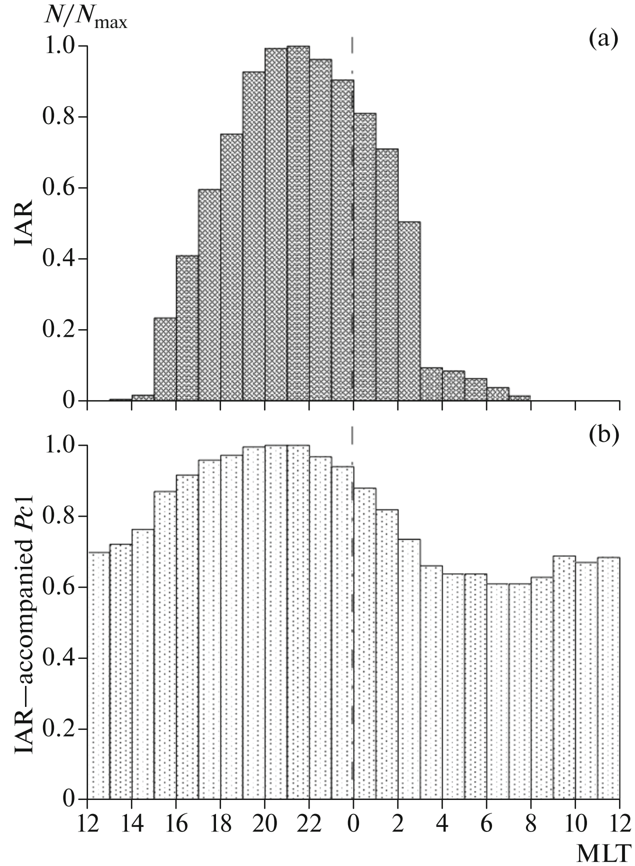

Fig. 3. Diurnal variations in the normalized number of events N/N_{max} of (a) IAR and (b) IARs accompanied by excitation of *Pc*1 pulsations.

occurrence almost during three 11—year cycles of solar activity (from the end of cycle 21 through cycle 24) and to compare it with the variation in the parameters of solar wind and IMF. This long-term IAR-recording series (about 30 years of observations) is studied for the first time. We note that the IAR analysis in previous studies (Belyaev et al., 2000; Baru et al., 2014) was were performed only for a single cycle of solar activity (~10—11 years).

As the main characteristics of the interplanetary medium, we analyzed the parameters of solar wind plasma and IMF, which were derived via the combination of several parameters, such as density, velocity, temperature, and others. In our opinion, parameter combinations best characterize the state of the magnetosphere and the processes occurring in it. For these parameters, we considered the ratio of proton density to the density of helium ions (α particles) Np/Na, the dynamic pressure of solar wind $P_{dyn} = \rho V^2$ (ρ is the plasma density, V is the velocity), and the parameter β, which characterizes the ratio of thermal pressure to the magnetic pressure, $\beta = NpkT/(B^2/8\pi)$, where Np is the proton density, T is the proton temperature, and B is the magnetic field value. In the OMNI database, the ratio of the density of α particles to the proton density Na/Np is presented. For convenience of comparisons, we used the parameter Np/Na, equal to $1/(Na/Np)$.

Figure 5 presents (a) the annual average values of the Wolf number; the annual number of IAR occurrences N of the (b) first and (c) second groups; and the annual average values of (d) the ratio Np/Na, (e) the dynamic pressure of solar wind P_{dyn}, and (f) the parameter β for two observation intervals from 1984 to 1993 and from 1997 to 2016. Figure 5b shows that the highest probability of observation of first-group IARs in both time intervals falls in years of solar activity minima (1985—1987 and 2008—2009, respectively). In the years of solar activity maxima (cycles 22—24), the probability of IAR observation is considerably lower, i.e., there is an explicit inverse dependence between the rate of IAR observation and solar activity. The detected regularity of the IAR behavior in the cycle of solar activity agrees with the IAR variation obtained based on data from midlatitude (Belyaev et al., 2000) and high-latitude (Baru et al., 2014) IAR observations. It should be noted that the IAR distribution shapes in

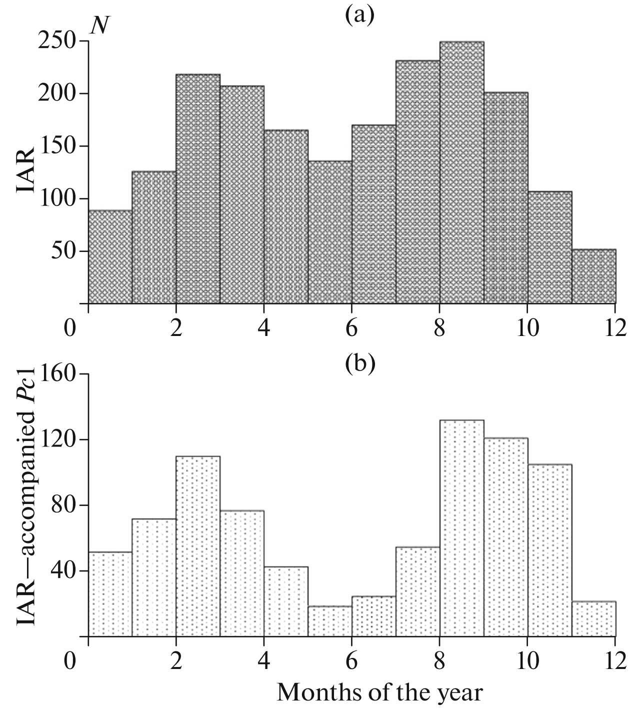

Fig. 4. Seasonal variations in the number of events N of (a) IAR and (b) IARs accompanied by excitation of $Pc1$ pulsations.

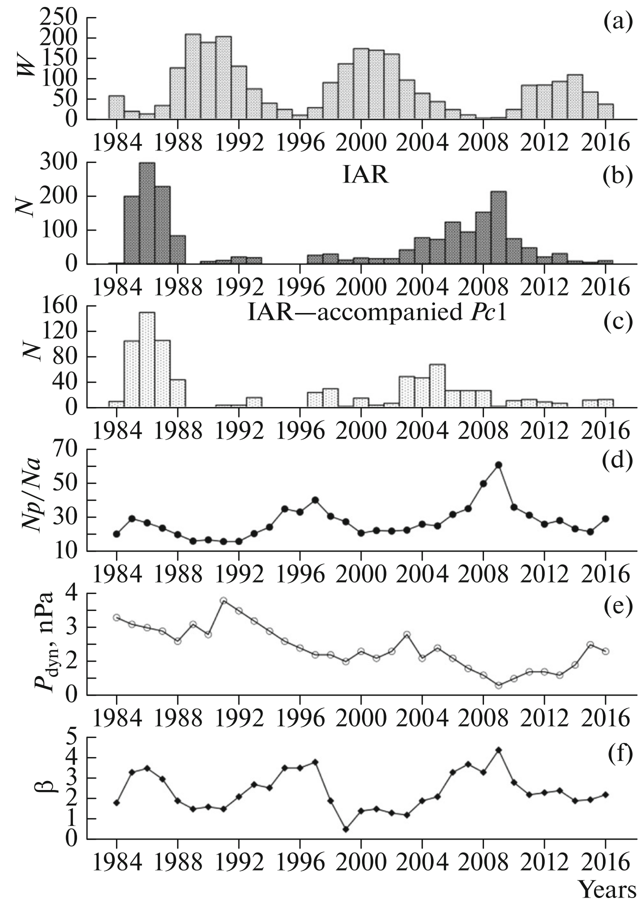

Fig. 5. Cyclic variations in the (a) solar activity (Wolf numbers, W); (b, c) number of observed events N of IAR of the (b) first and (c) second groups; (d) ratio of the number of protons to helium ions Np/Na; (e) dynamic pressure of solar wind P_{dyn}; (f) parameter β at the end of solar cycle 21 through cycle 24.

the first and second intervals considerably differ. Thus, in the interval 1984–1993, an abrupt growth in the number of IAR occurrences and then their subsequent sharp decrease are observed. In other words, the IAR distribution has a peaked shape. In the interval 1997–2016, a smooth growth in the number of occurrences reaches a maximum and then gradually decreases, which is characteristic of the IAR distribution shape. The presence of different shapes of distributions of the IAR number in different time intervals may be evidence not only of their 11-year cyclicity but also of 22-year cyclicity.

The cyclic variation of second-group IARs (accompanied by pearls) in the interval of 1984–1993 is similar to the variation of the first-group IARs (Fig. 5c). The maximum rate of their occurrence is marked also in years of minimal solar activity. In the other time interval (1997–2016), the IAR dynamics of the two groups differs fundamentally. Thus, the maximum rate of observation of IARs accompanied by $Pc1$ pulsations falls within the decay of solar cycle 23 (Fig. 5c) rather than on its minimum. We turn our attention to the fact that a deviation from the regularity (the highest and lowest probabilities of IAR observation are observed at the solar activity minimum and maximum, respectively) arises only when the IARs are accompanied by pearls. The known inverse dependence of activity of $Pc1$ pulsations on the number of sunspots is violated in odd cycles of solar activity (Matveeva, 1987). For example, for the odd solar cycle 19, the maximal $Pc1$ activity is typically on its declining phase (Matveeva, 1987). A specific feature of the dynamics of the IARs accompanied by pearls may likely be associated with the specific features of even and odd cycles, the same as the variation in $Pc1$ pulsations in the solar cycle.

Comparison of the dynamics of the number of the first-group IAR observations with variation in the parameter Np/Na has shown that the IAR maximum coincides with the maximum value of the ratio of proton density to the density of helium ions in the solar wind, both in solar cycles 21 and 23. A decrease in the solar-wind parameter Np/Na leads to a reduction (while its growth leads to an increase) in the probability of IAR observation (Fig. 5d). With a value of $Np/Na \sim 10$–20, the probability of IAR observation is significantly lower than with $Np/Na \sim 50$–60. This, in turn, implies that the maximum proton density in comparison to the helium ion density in the years of the solar activity minimum is the significant factor for IAR excitation. Another factor having an effect on the appearance of resonance bands of the spectrum may be the dynamic pressure of the solar wind. Antiphase behavior is observed between the dynamics of IAR emission and $P_{\rm dyn}$ variations in the solar cycle. The maximum rate of IAR emission observation is noted at the decreased dynamic pressure of solar wind (Fig. 5e). Since the degree of magnetosphere compression by the solar wind depends on the dynamic pressure, then it can be noted that the probability of observation of the IAR emission has the maximum value when the magnetosphere is not compressed. Additionally, the probability of IAR observation is high when parameter β reaches maximum values (Fig. 5f), i.e., the thermal pressure of the plasma considerably (4–5 times) exceeds the magnetic pressure.

The dynamics of IARs accompanied by excitation of *Pc*1 pulsations in cycle 21 coincides with the variation in the ratio Np/Na and in parameter β, but it is antiphased relative to the $P_{\rm dyn}$ variation similarly to events of the first group (Figs. 5c–5f). However the correspondence between the probability of observation of the second-group IAR and the parameters Np/Na, $P_{\rm dyn}$ and β is violated in cycle 23. The maximal probability of IAR occurrence falls within the growth phase of the ratio Np/Na and the decay phase of $P_{\rm dyn}$ in the solar cycle rather than on their maximum and minimum, respectively. Similar regularities are detected in the comparison of the second-group IAR radiations with the behavior of parameter β during the interval 1997–2016. The maximum number of occurrences of the IARs accompanied by pearls does not coincide with the peak of parameter β. Thus, IARs observed synchronously with pearls have certain specific features in solar cycle 23.

4. DISCUSSION

As a result of the research, two groups of IAR emissions are identified, one of which has a close relation to the excitation of pearls. It was detected that certain specific features of *Pc*1 pulsations reveal themselves in the IAR behavior. It was recognized in the dynamics of the resonance band frequency, the distribution of IAR observation time, and their diurnal, seasonal, and cyclic variations. For example, the observation duration of IARs accompanied by pearl excitation is significantly longer than the observation duration of IARs without pearls (see Fig. 2). In our opinion, the longer observation duration intervals of the second-group IARs are caused by processes that accompany pearl excitation.

The regularities of the diurnal and cyclic variations in the probability of IAR observation that we obtained coincide in many respects with results of other authors. At the same time, the dependence of the probability of the observation of two IAR groups on the season (see Fig. 4) differs fundamentally from the seasonal variation of other authors, e.g., (Baru et al., 2013; Polyushkina et al., 2015). Disagreements in the conclusions on IAR seasonal variation may be associated with the fact that the dependences of the probability of the observation of both midlatitude and high-latitude IARs on the season were constructed (Baru et al., 2013; Polyushkina et al., 2015) on the basis of either episodic data or a limited number of observation data. We derived the seasonal variation in the number of observations (of IARs and the IARs accompanied by pearl excitation) based on a much larger set of statistical material (about 3000 days of IAR observations) than in other studies. This allows us to assert that the probability of IAR observation has a seasonal behavior with a maximum in the season of equinoxes (Fig. 4) rather than in the winter season. It is characteristic that the shape of the dependence of the number of observations of two IAR groups on the season coincides with the semiannual variation in the geomagnetic activity, which has maxima in periods of equinoxes (Danilov et al., 2013). Thus, the IAR seasonal variation can be assumed to be caused by some other factors rather than by the effect of the local ionospheric state on the probability of IAR observation (Baru et al., 2013). These factors may include the effect of the angle of the slope of the geomagnetic dipole of the Earth to the Sun–Earth line, the change in the heliolatitude of the Earth, or processes in the magnetosphere tail (Danilov et al., 2013). Here, it should be noted that a maximum during equinoxes is also characteristic of the seasonal distribution of the rate of occurrence of *Pc*1 pulsations (Pudovkin et al., 1976). The coincidence of the seasonal variation of IAR and *Pc*1 pulsations may indirectly indicate the link between these ULF pulsations.

It is emphasized in many publications that ionospheric local conditions are the decisive factor in the formation of spectrum resonance structures and determine their properties. The results of our research and those of Guglielmi and Potapov (2017) have shown that the interplanetary medium state also affects the activity of IAR emission. As mentioned above, the highest probability of recording of two IAR groups falls in years of reduced values of the dynamic pressure of solar wind (Fig. 5e). It is known that a reduction in dynamic pressure leads to a situation in which the plasmapause and radiation belts move away from the Earth. These magnetosphere regions determine the generation of ion-cyclotron waves. In addition, there is a sufficiently good correlation of the variation in IAR observation with the ratio of proton density to the helium ion density Np/Na and with parameter β in the solar cycle (Figs. 5d, 5f). The larger is the excess density of solar wind protons over the density of helium ions, the higher is the IAR excitation probability. In years when the solar activity has the maximum value, the proton density in the smaller degree dominates over the α-particle density and the

IAR statistics considerably decreases. Earlier, (Matveeva and Shchepetnov, 2006), attention was paid to a similar dependence of the cyclic variation in the activity of *Pc*1 geomagnetic pulsations on the *Np*/*Na* value. Thus, the arrival of solar wind protons controls the cyclic variation in the emission of both IARs and pearls, for which the inverse dependence of activity on the Wolf numbers is also typical (Matveeva et al., 1972). The seasonal behavior of the observation probability of two IAR groups with equinoctial maxima, as well as the correlation of IAR observation variation with the ratio of proton density to helium ion density (*Np*/*Na*) in the solar cycle make it impossible to draw an unambiguous conclusion about the fact that resonance structures are defined only by ionospheric plasma properties.

Earlier (Trakhtengerts et al., 2000), the feedback of the probability of the observation of IARs and *Pc*1 pulsations with solar activity was interpreted based on the role of the ionospheric Alfvén resonator in the formation of both modes of electromagnetic oscillations. However, a specific feature of the IAR and *Pc*1 behavior was detected in this work and already in an earlier study (Dovbnya et al., 2012): the dynamics of the change in the characteristic frequency (at which pearls are observed) in the overwhelming majority of cases coincides with the dynamics of the first harmonic of IAR emission. The frequency of the IAR fundamental mode is proportional to the electron number density N_e, an indicator of which is the critical frequency of the ionospheric F_2 layer (Polyakov and Rapoport, 1981). This conclusion is confirmed in a number of works (e.g., Baru et al., 2014; Polyushkina et al., 2015). On the other hand, *Pc*1s arise in the outer radiation belt of the Earth due to the development of the ion-cyclotron instability and propagate in the magnetosphere along geomagnetic field lines (Guglielmi and Troitskaya, 1973). The *Pc*1 pulsation frequency is close to the proton gyrofrequency in the equatorial plane of the magnetosphere. Since *Pc*1 is assumed to relate to the cyclotron instability, then the carrier frequency at which pearl generation occurs is proportional to the magnetic field in the equatorial neighborhood of the magnetosphere. Thus, the formation of the frequency composition of pearls to a large extent is controlled by dynamics of the magnetosphere rather than by the ionosphere dynamics. Since the dynamics of the spectral band frequency is closely related to the dynamics of *Pc*1 frequency, then IAR generation can be assumed to be associated with protons of radiation belts.

A major factor influencing the process of excitation and propagation of *Pc*1 pulsations is the density of solar wind protons (Matveeva et al., 1972; Matveeva and Shchepetnov, 2006). The association of *Pc*1 pulsation excitation with proton precipitations was shown experimentally in many works (e.g., Yahnina et al., 2000). We revealed that emissions with a spectrum resonance structure and a series of pearls are observed synchronously in 30% of events. In this case, pearls are recorded at the frequency of the first IAR harmonic. Moreover, the behavior of IARs and *Pc*1 frequencies is the same in 80% of events. This experimental fact is evidence that the link between these two phenomena is noncasual. Here, a work by Fedorov et al. (2016) should be noted. They developed a theoretical model of the interaction between magnetospheric Alfvén waves and the ionosphere. According to numerical simulation (Fedorov et al., 2016), the transmittance factor of the ionosphere has a maximum at the IAR fundamental frequency and first harmonic frequency at night time, which may allow an understanding of the close relationship (that we detected) between the dynamics of IARs and *Pc*1 frequencies.

Since the role of solar wind protons in the generation of *Pc*1 pulsations is theoretically substantiated and experimentally demonstrated, and the frequency of the IAR first resonance band coincides with the *Pc*1 frequency, then the effect of solar wind protons on the IAR generation probably cannot be excluded. Another indication of the possible role of protons in IAR excitation is the following. In the course of research, we found that pearls are observed concurrently with IARs in most occurrences (75%); only in 25% are pearls recorded on the earth surface without IARs. Comparison of the cyclic variations of second-group IARs and pearls revealed the following regularities. Thus, the maximum probability of the occurrence of IARs accompanied by pearls is observed in 2005 (see Fig. 5c). Figure 6 presents the cyclic variation in solar activity (the annual average values of Wolf numbers *W*) and the dynamics of the number of occurrences (*N*) of pearls (the unstructured *Pc*1 pulsations were beyond our consideration) obtained based on the dynamic spectra of ULF pulsations and analog records of the magnetic field for 1984–2016. It can be seen that the maximum probability of pearls in solar cycle 23 falls within the decline phase of solar activity, i.e., 2005 (Fig. 6b). Thus, the dynamics of a IAR accompanied by pearls and the variation of series of pearls in solar cycle 23 coincide. At the same time, the maximum observation of the IARs without pearls, in contrast to the events of the first group, corresponds to the minimum (2009) of solar activity (Fig. 5c). The coincidence of the statistics of observations of IARs and pearls in solar cycles 21 and 23 is also indirect evidence of the link between these oscillatory processes.

In the context of this work, while by no means denying the role of IARs in the formation of resonance bands, we wanted to pay attention to the close relation between IARs and *Pc*1 pulsations and also to the interplanetary medium parameters that affect the excitation of these two wave processes. Even if IARs and *Pc*1s are not genetically related, their joint excitation is defined by the dynamics of structural formations of the magnetosphere, which, in turn, is controlled by the interplanetary medium parameters. In particular, the role of these parameters can be played by the ratio

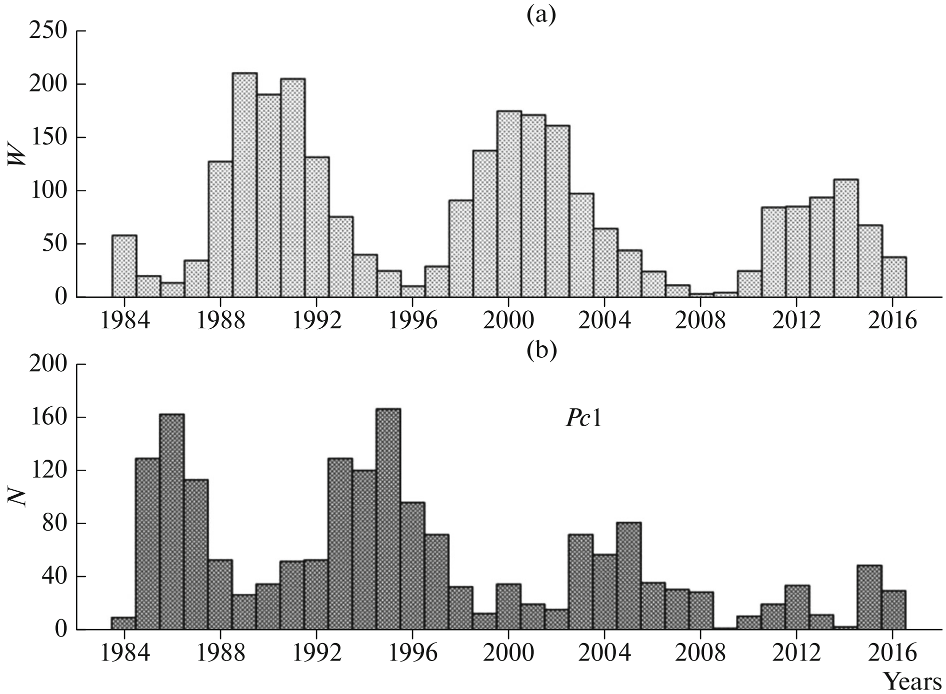

Fig. 6. Cyclic variation in (a) Wolf numbers *W* and (b) the number of pearl observations *N* at the midlatitude Borok observatory.

of proton density to helium ion density (Np/Na), the dynamic pressure of solar wind, and parameter β. At the same time, the revealed specific features of IAR and *Pc*1 behavior do not allow an unambiguous selection to be made with respect to the structural region of the magnetosphere in which IAR emission can be generated.

5. CONCLUSIONS

The results of our research showed that IARs are accompanied in 30% of events by the simultaneous observation of structured *Pc*1 geomagnetic pulsations and IARs without excitation of pearls are observed in 70% of events. A characteristic specific feature of pearls is the fact that they are recorded predominantly at the frequency of the IAR first resonance band. The qualitative coincidence of the dynamics of frequencies of IARs and *Pc*1 wave packets is detected in 80% of events. The maximum probability of IAR observation falls in the premidnight hours (2000–2200 MLT). The IAR seasonal variation is characterized by the presence of two equinoctial maxima. It is shown that the 11-year variation in the IAR radiation is controlled by the dynamics of some parameters of the solar wind and IMF. The probability of IAR observation has a maximum value (in years of solar activity minimum) when the ratio of the proton density to the density of helium ions (α particles) Np/Na and the parameter β (which characterizes the ratio of thermal pressure to magnetic pressure) reach maximum values, while the dynamic pressure of solar wind P_{dyn} (which controls the magnetosphere compression) is reduced. The pearl properties were found to have an effect on IAR behavior regularities. The coincidence of the dynamics of frequencies of the IAR first resonance band and pearls (as well as of their seasonal and cyclic variations) may be evidence of the interrelation of these oscillatory processes and the possible common mechanism of their generation.

ACKNOWLEDGMENTS

This work is fulfilled according to the subject "Influence of Space Factors on Development of Extreme Processes in the Magnetosphere of the Earth" (government contract no. 0144-2014-00116).

REFERENCES

Baru, N.A., Koloskov, A.V., and Rakhmatulin, R.A., Dependence of the characteristics of ionospheric Alfvén resonance on the geospace state according to data from synchronous measurements in Antarctica and Eurasia, *Ukr. Antarkt. Zh.*, 2013, no. 12, pp. 177–185.

Baru, N.A., Koloskov, A.V., Yampol'skii, Yu.M., Rakhmatulin, R.A., and Pashinin, A.Yu., Observability of ionospheric Alfvén resonances in Antarctica in a complete cycle of solar activity and the splitting effect, *Ukr. Antarkt. Zh.*, 2014, no. 13, pp. 124–132.

Belyaev, P.P., Polyakov, S.V., Rapoport, V.O., Trakhtengerts, V.Yu., Detection of resonance structure in the atmospheric electromagnetic noise background spectrum in the range of short-period geomagnetic pulsations, *Dokl. Akad. Nauk SSSR*, 1987, vol. 297, pp. 840–843.

Belyaev, P.P., Polyakov, S.V., Rapopopt, V.O., and Trakhtengerts, V.Yu., Experimental studies of the spectral resonance structure of the atmospheric electromagnetic noise background within the range of short-period geomagnetic pulsations, *Radiophys. Quantum Electron.*, 1989a, vol. 32. no. 6, pp. 491–501.

Belyaev, P.P., Polyakov, S.V., Rapoport, V.O., and Trakhtengerts, V.Yu., Theory for the formation of resonance structure in the spectrum of atmospheric electromagnetic background noise in the range of short-period geomagnetic pulsations, *Radiophys. Quantum Electron.*, 1989b, vol. 32, no. 7, pp. 594–601.

Belyaev, P.P., Bosinger, T., Isaev, S.V., and Kangas, J., First evidence at high latitudes for the ionospheric Alfvén resonator, *J. Geophys. Res.: Space*, 1999, vol. 104, no. A3, pp. 4305–4317.

Belyaev, P.P., Polyakov, S.V., Ermakova, E.N., and Isaev, S.V., Solar cycle variations in the ionospheric Alfvén resonator 1985–1995, *J. Atmos. Sol.-Terr. Phys.*, 2000, vol. 62, pp. 239–248.

Bosinger, T., Haldoupis, C., Belyaev, P.P., Yakunin, M.N., Semenova, N.V., Demekhov, A.G., and Angelopoulos, V., Spectral properties of the ionospheric Alfvén resonator observed at a low-latitude station (L = 1.3), *J. Geophys. Res.: Space*, 2002, vol. 107, no. A10, pp. SIA4-1–SIA4-9.

Danilov, A.A., Krymskii, G.F., and Makarov, G.A., Geomagnetic activity as a reflection of processes in the magnetospheric tail: 1. The source of diurnal and semiannual variations in geomagnetic activity, *Geomagn. Aeron. (Engl. Transl.)*, 2013, vol. 53, no. 4, pp. 441–447.

Dovbnya, B.V., Zotov, O.D., Klain, B.I., Kurazhkovskaya, N.A., Potapov, A.S., and Rakhmatulin, R.A., Spectral properties of the Pc1 waves and noise-like pulsations with resonance structure, in *Book of Abstracts 9th International Conference "Problems of Geocosmos"*, St. Petersburg, 2012, p. 164.

Dovbnya, B.V., Guglielmi, A.V., Potapov, A.S., and Klain, B.I., On the existence of an over-ionospheric Alfvén resonator, *Soln.-Zemnaya Fiz.*, 2013, no. 22, pp. 12–15.

Dovbnya, B.V., Potapov, A.S., Guglielmi, A.V., and Rakhmatulin, R.A., On influence of MHD resonators upon geomagnetic pulsations, *Geofiz. Zh.*, 2014, vol. 36, no. 6, pp. 143–152.

Dudkin, D., Pilipenko, V., Korepanov, V., Klimov, S., and Holzworth, R., Electric field signatures of the IAR and Schumann resonance in the upper ionosphere detected by Chibis-M microsatellite, *J. Atmos. Sol.-Terr. Phys.*, 2014, vol. 117, pp. 81–87.

Fedorov, E., Mazur, N., Pilipenko, V., and Engebretson, M., Interaction of magnetospheric Alfvén waves with the ionosphere in the Pc1 frequency band, *J. Geophys. Res.: Space*, 2016, vol. 121, pp. 321–337. doi 10.1002/2015JA021020

Guglielmi, A.V. and Potapov, A.S., Influence of the interplanetary magnetic field on ULF oscillations of the ionospheric resonator, *Cosmic Res.*, 2017, vol. 55, no. 4, pp. 248–252.

Guglielmi, A.V. and Troitskaya, V.A., *Geomagnitnye pul'satsii i diagnostika magnitosfery* (Geomagnetic Pulsations and Diagnostic of the Magnetosphere), Moscow: Nauka, 1973.

Kerttula, R., Mursula, K., Pikkarainen, T., and Kangas, J., Storm-time Pc1 activity at high and middle latitudes, *J. Geophys. Res.*, 2001, vol. 106, no. A4, pp. 6213–6227.

Lysak, R.L., Feedback instability of the ionospheric resonant cavity, *J. Geophys. Res.*, 1991, vol. 96, pp. 1553–1568.

Matveeva, E.T., Cyclic variation of the activity of *Pc*1-type geomagnetic pulsations, *Geomagn. Aeron.*, 1987, vol. 27. no. 3, pp. 455–458.

Matveeva, E.T. and Shchepetnov, R.V., Interrelation of the activity of ion-cyclotron waves in the Earth's magnetosphere with parameters of the solar wind, *Cosmic Res.*, 2006, vol. 44, no. 6, pp. 548–550.

Matveeva, E.T., Kalisher, A.L., and Dovbnya, B.V., Physical conditions in the magnetosphere and interplanetary space during the excitation of *Pc*1-type geomagnetic pulsations, *Geomagn. Aeron.*, 1972, vol. 12, no. 6, pp. 1125–1127.

Parkhomov, V.A., Tsegmed, B., and Dmitriev, A.V., On the origin of a burst of unstructured Pc1 pulsations according to simultaneous observations from the ground and geostationary orbit, *Soln.-Zemnaya Fiz.*, 2013, no. 23, pp. 75–83.

Pokhotelov, O.A., Khruschev, V., Parrot, M., Senchenkov, S., and Pavlenko, V.P., Ionospheric Alfvén resonator revisited: Feedback instability, *J. Geophys. Res.*, 2001, vol. 106, no. A11, pp. 25813–25824.

Polyakov, S.V. and Rapoport, V.O., Ionospheric Alfvén resonator, *Geomagn. Aeron.*, 1981, vol. 21, pp. 816–822.

Polyushkina, T.N., Dovbnya, B.V., Potapov, A.S., Tsegmed, B., and Rakhmatulin, R.A., Frequency structure of IAR spectral bands and ionosphere parameters, *Geofiz. Issled.*, 2015, vol. 16, no. 2, pp. 39–57.

Potapov, A.S., Polyushkina, T.N., Oinats, A.V., Pashinin, A.Yu., Raita, T., and Tsegmed, B., The first attempt to estimate the ion content over the ionosphere using data from the IAR frequency structure, *Sovrem. Probl. Distantsionnogo Zondirovaniya Zemli Kosmosa*, 2016, vol. 13, no. 2, pp. 192–202.

Pudovkin, M.I., Raspopov, O.M., and Kleimenova, N.G., *Vozmushcheniya elektromagnitnogo polya Zemli* (Disturbances in the Earth's Electromagnetic Field), vol. 2: *Korotkoperiodicheskie kolebaniya geomagnitnogo polya* (Short-Period Oscillations in the Geomagnetic Field), Leningrad: Izd. LGU, 1976.

Surkov, V. and Hayakawa, M., Ionospheric Alfvén Resonator (IAR), in *Ultra and Extremely Low Frequency Electromagnetic Fields*, Tokyo: Springer, 2014, pp. 145–207. doi 10.1007/978-4-431-54367-1_5

Surkov, V.V., Pokhotelov, O.A., Parrot, M., Fedorov, E.N., and Hayakawa, M., Excitation of the ionospheric resonance cavity by neutral winds at middle latitudes, *Ann. Geophys.*, 2004, vol. 22, no. 8, pp. 2877–2889.

Trakhtengerts, V.Y., Demekhov, A.G., Belyaev, P.P., Polyakov, S.V., Ermakova, E.N., and Isaev, S.V., A mechanism of anticorrelation in the occurrence of ULF electromagnetic noise resonance structure and *Pc*1magnetic pulsations through the solar activity cycle, *J. Atmos. Sol.-Terr. Phys.*, 2000, vol. 62, pp. 253–256.

Yahnin, A.G., Semenova, N.V., Ostapenko, A.A., Kangas, J., Manninen, J., and Turunen, T., Morphology of the spectral resonance structure of the electromagnetic background noise in the range of 0.1–4 Hz at L = 5.2, *Ann. Geophys.*, 2003, vol. 21, no. 3, pp. 779–786.

Yahnina, T.A., Yahnin, A.G., Kangas, J., and Manninen, J., Proton precipitation related to *Pc*1 pulsations, *Geophys. Res. Lett.*, 2000, vol. 27, no. 21, pp. 3575–3578.

Translated by M. Samokhina